Penerbit Akademia Baru

CFD Letters

Journal homepage: www.akademiabaru.com/arbb.html
ISSN: 2180-1363

Study On the Effects of Rotational and Transverse Speed On Temperature Distribution Through Friction Stir Welding of AA2024-T3 Aluminum Alloy

Open Access

Nageeb Salman Abtan[1], Ataalah Hussain Jassim[1,*], Mustafa Shakir Marmoos[1]

[1] Department of Mechanical Engineering, Tiktit University, College of Engineering, Iraq

ARTICLE INFO

Article history:
Received 20 November 2018
Received in revised form 30 December 2018
Accepted 4 January 2019
Available online 11 January 2019

Keywords:
Friction stirs welding; Temperature distribution; Numerical; Simulation.

ABSTRACT

A nonlinear three-dimensional thermal process was studied experimentally and numerically. The present study aims to investigate the distribution of temperature in the joint of aluminum AA2024-T3 plates throughout the friction stirred butt. The experiments were conducted at a constant tool tilted angle of 3° under various rotational speeds (690, 1130, 2000 rpm) and feed rates (20, 32, 45 mm/min). The highest temperature of 860 K was obtained at the experimental condition of 2000 rpm, 20 mm/min, 20 dwell times, and 3° tilt angle. This value was less than the melting point temperature of Al 2024 alloy (911 K). The comparison between the numerical and experimental results of temperature distribution showed a good agreement. The deviation between the theoretical and experimental results for the maximum and minimum rotational speed and feed rate was (7, 10 %) and (5, 12 %), respectively.

1. Introduction

Aluminum alloy has unique properties such as strength/weight, good machinability, corrosion resistance, etc. These characteristics have led to increased demand for this alloy, especially in the aerospace sector. However, it is difficult to join these alloys by fusion welding because of their low melting point and the presence of an oxide layer. In addition, more defects are encountered during welding, such as porosity and distortion [1-4]. Friction-Stir Welding (FSW) is a new joining method that was patented in The Welding Institute (TWI), Cambridge, UK (1991). The process is a solid-state technique as illustrated in Figure 1. Heat is generated in this method by the friction between the welding tool and workpiece; the welding tool is equipped with a pin or a probe which is plunged into the butted plate and pin shoulder [5-10]. The tool is characterized as non-consuming and non-melting during the process. The FSW process has presented as a solution to the problems encountered during the welding of aluminum alloys [11-17].

* *Corresponding author.*
Email address: ataalahhussain@gmail.com (Ataalah Hussain Jassim)

The softened materials around the pin and beneath the shoulder produce a solid-state welding by motion tool (rotational and welding speed). It is expected that this process will inherently produce a weld with that lowers the residual stress and distortion as compared to the fusion welding methods since no melting of the material occurs during the welding [18-22]. The FSW process parameters can be classified into three groups: (1) tool-related parameters (includes pin and shoulder materials, pin and shoulder diameter, pin length, thread pitch, and feature geometry); (2) Machine-related parameters (includes welding and rotational speed, tool tilt angle, and plunge force; (3) other parameters (includes anvil material and size, workpiece size and properties, etc.) [8]. The diagram of the FSW process parameters was shown in Figure 2.

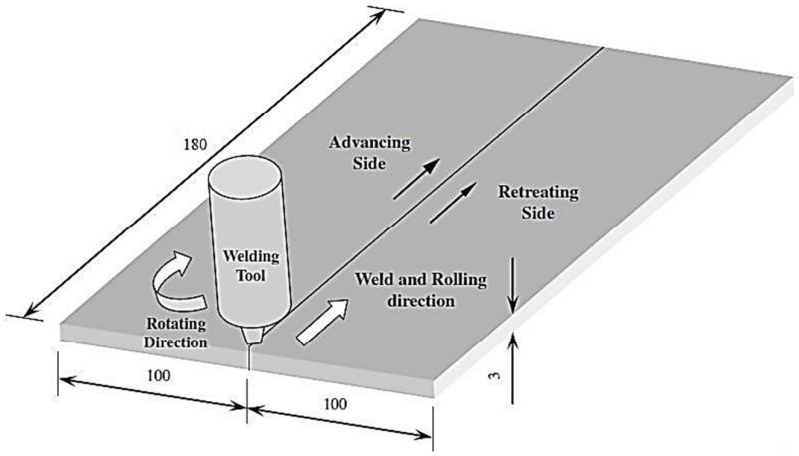

Fig. 1. Schematic diagram of the principle of the FSW process and terminology

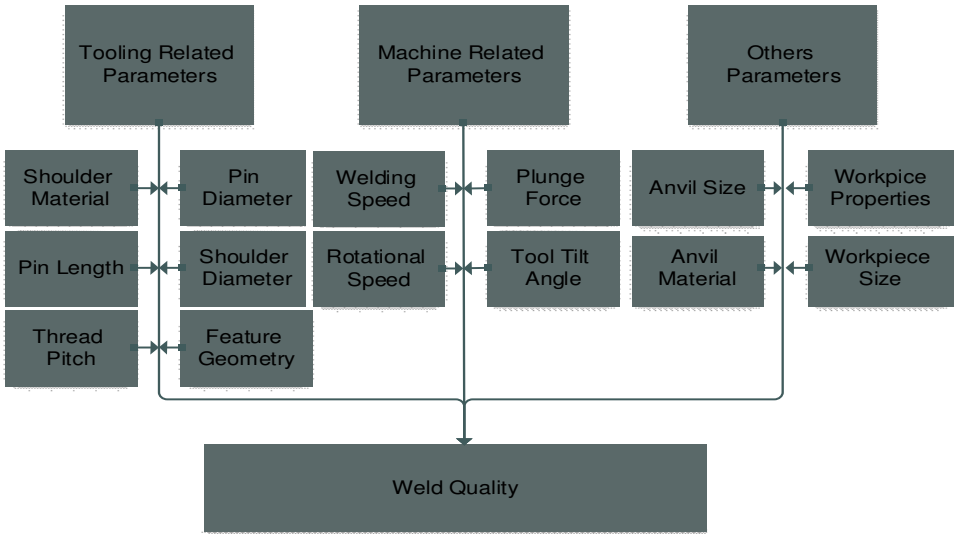

Fig. 2. Schematic diagram of the effect of FSW process parameters

After the FSW technique was patented by TWI, many researchers have studied the mechanical and metallurgical behavior of friction stir welded joints. It is obvious from the literature that most of the studies focused on the FSW of aluminum alloys such as AA6061, AA6083, AA7075, etc. because of their application in the aerospace industry [23-27]. In addition, most of the existing studies investigated the mechanical properties and microstructure of FSW joints but failed to provide information about the process temperature distribution [28, 29].

Song *et al.,* [30] have developed a 3D model with a moving coordinate system for describing the heat transfer during FSW processes. The model helped to find the temperature distribution of AA6061 near the tool. Also, they concluded that preheating is advantageous for FSW. Aval *et al.,* [31] have experimentally and numerically (3D finite element) studied heat transfer through FSW. The result showed temperature distribution on the advancing side more than the retreating side. Muhsin *et al.,* [32] measured the thermal distribution through FSW of AA7020-T53 alloy. The results showed that the temperature distribution is symmetrical with respect to the welding line. The numerical results found the temperature to increase with increased rotational speed and decreased welding speed. The numerical result agreed with the measured data with a relative error ratio of 2 %. Padmanaban *et al.,* [33] used CFD to investigate temperature distribution and materials flow during the FSW process for two alloys (AA2024 and AA7075). They found increases in the rotational speed and shoulder diameter to increase the temperature while increases in the welding speed decreased the temperature. Ghetiye *et al.,* [34] investigated the formation of defects in FSW butt joints under different welding conditions for alloy (AA8011). They FSW experiments were conducted in air and immersed conditions. Also, they found a superior strength in the immersed case compared to the air process.

Jain *et al.,* [35] have studied the thermal profile of alloy AA2024 and reported that the maximum temperature was attained in the nugget zone while the temperature profile assumed a 'V' shape due to higher heat generation on the top surface compared to the bottom. Also, they found the deformation to increase with increases in the rotational speed of the tool but decreases with increase welding speed. Aziz *et al.,* [36] experimentally and numerically (finite element) studied temperature distribution for AA2219 alloy. The results showed the temperature field obtained from the FE simulations to be similar to the temperature field obtained experimentally, with a maximum relative error of 7 %. Also, they found that a high rotational speed caused a higher amount of frictional heat and plastic dissipation energies. Verma *et al.,* [37] experimentally studied the FSW of AA6082 alloy and found the temperature on the advance side to be more compared to the retreating side for the investigated working conditions. The maximum temperature was obtained at the working condition of 2º tilt angle, 30 dwell time, 500 rpm, and 20 mm/min. Also, the temperature was found to increase with the dwell time.

The aim of this study is to numerically and experimentally investigate the thermal distribution during the friction stir welding (FSW) of AA2024-T3 aluminum alloy with emphasis on the effect of machine parameters (welding transverse and rotational) speed on the temperature distribution during the process. For the verification of the numerical predictions, the numerical results were compared with the experimental data.

2. Experimental Details

In this study, AA2024-T3 plate (dimension = 170 mm × 100 mm × 3 mm) was selected as the weld material. Two plates were prepared in a universal milling machine and fixed to a backing plate which served as a support during the FSW process. The tool pins were designed and manufactured from tool steel as shown in Figure 3. The temperature properties of AA2024-T3 aluminum alloy at different temperatures were given in Figure 4. Four k-type thermocouples were placed at equal distance from the weld line to measure the temperature along the advancing side (AS); the thermocouples were placed on the AS because many researchers have found the temperature at the AS to be higher than at the retreating side (RS). A data logger thermometer (Applent AT 4808) with 8 channels (Figure 5) was used for measuring the temperature distribution during the FSW process. The data logger records the process temperature and produces the results as an excel file.

One thermocouple was placed 10 mm from the center line and 1.5 mm depth from the top surface. Figure 6 showed the position of the thermocouple in the weld line.

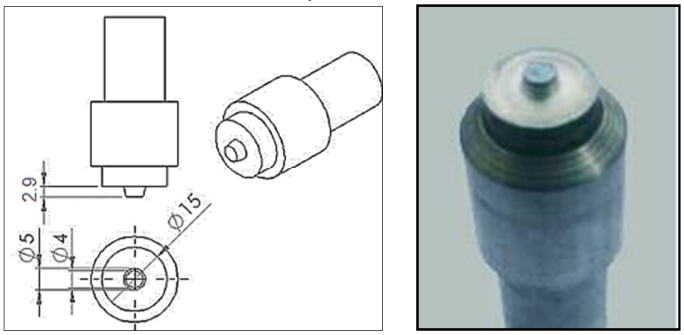

Fig. 3. The tapered pin tool (all dimension in mm)

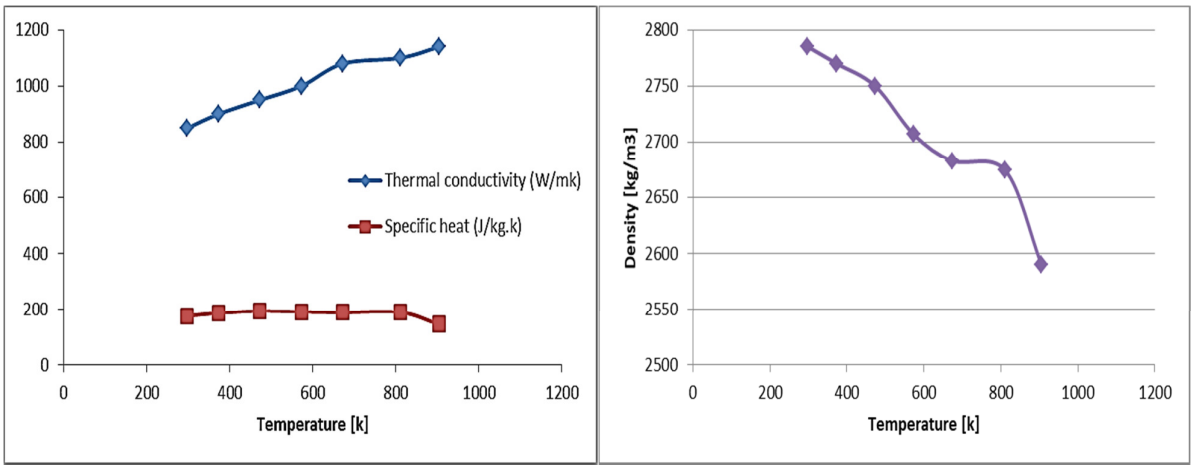

Fig. 4. Thermal materials properties of AA2024-T3

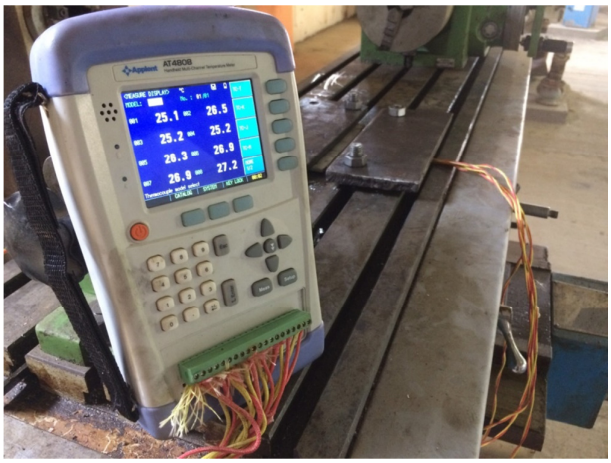

Fig. 5. The data logger used in measuring temperature

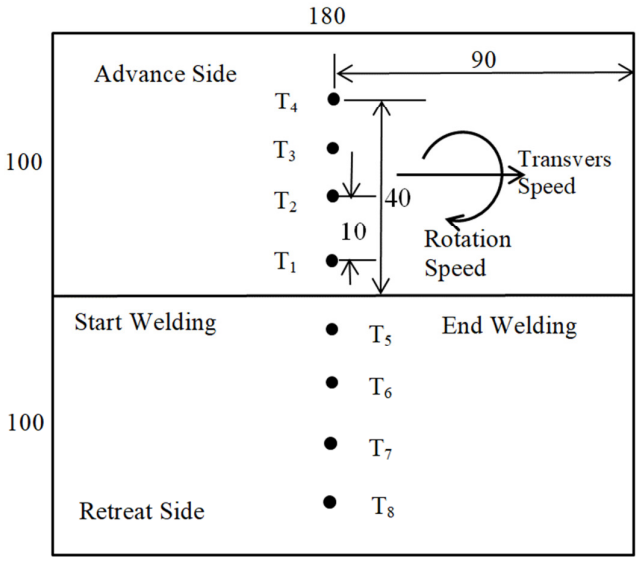

Fig. 6. Schematic diagram shows the position of thermocouple along advancing side (All dimensions in mm)

The parameters were implemented at a constant tilt angle and dwell time with different rotational and welding speeds. The parameters used are presented in Table 1.

Table 1
Machine parameters used in this study

Sample No.	Rotational speed (rpm)	Welding speed (mm/min)	Dwell time (s)	Tilt angle (°)
1		20		
2	690	32		
3		45		
4		20		
5	1130	32	20	3
6		45		
7		20		
8	2000	32		
9		45		

3. Finite Element Thermal Model of FSW

The thermal model of the FSW process was investigated in this study using finite element simulation. The ANSYS Parametric design language (APDL) provided by ANSYS group® was used to build the finite element method in non-linear and transient three-dimensional heat transfer model to determine the temperature distribution [38-40]. The temperature was determined as a function of time and the coordinates x, y, and z. In addition, the model was validated by comparing the simulated results with the experimental data.

3.1 Thermal model

The purpose of the thermal model is to calculate the transient temperature distribution as a function of time (t) and spatial coordinates (x, y, z) using Eq. 1 [33]

$$\rho C \frac{\partial T(x,y,z,t)}{\partial t} = -\left(\frac{\partial R_x}{\partial x} + \frac{\partial R_y}{\partial y} + \frac{\partial R_z}{\partial z}\right) + Q(x,y,z,t) \quad (1)$$

where T is the temperature, ρ is the density, C is the specific heat, R is the heat flux per unit area. By applying Fourier's law $(R = k\frac{\partial T}{\partial n})$, Eq. 1 becomes

$$\rho C \frac{\partial T(x,y,z,t)}{\partial t} = -\left(\frac{\partial}{\partial x}\left(k_x \frac{\partial T}{\partial x}\right) + \frac{\partial}{\partial y}\left(k_y \frac{\partial T}{\partial y}\right) + \frac{\partial}{\partial z}\left(k_z \frac{\partial T}{\partial z}\right)\right) + Q(x,y,z,t) \quad (2)$$

where k is the thermal conductivity.

3.2 Assumptions

The following assumptions were developed from the finite element thermal model:

No melting of the workpiece the during FSW process.

I. Weld material is isotropic and homogeneous.
II. Boundary conditions are symmetrical around the center line of weld.
III. Heat transfer to the tool and machine is negligible.
IV. The process is a solid-state and no change in state.
V. Radiation by top surface.

3.3 Heat Generation

In FSW thermal model, there are two sources of heat inputs, 1) heat gendered at the tool shoulder-welds interface, and 2) heat generated at the tool pin-welds interface as shown if Figure 7.

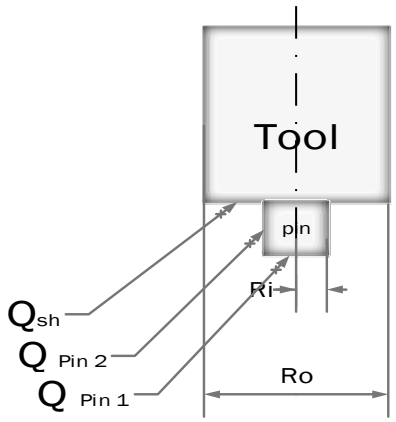

Fig. 7. Schematic of the region tool-weld interface

3.4 Heat Input at the Tool Shoulder-Weld Interface

The heat input at the tool shoulder-weld interface is assumed to be frictional heat and the local heat can be calculated from

$$Q_{Sh} = \frac{2}{3}(1-\delta)\pi\mu p\omega(R_{sh}^3 - R_p^3) \quad (3)$$

where δ is the slip factor which has been reported to be between 0.6 – 0.85, μ is the friction coefficient found to be between 0.3 – 0.5 [41, 42], ω is the rotational speed, p is the pressure, R_{sh} is the radius of the shoulder, and R_p is the radius of a pin.

3.5 Heat Input at the Tool Pin-Weld Interface

The heat input at the tool pin-weld interface is in two parts; 1) feat generated by the friction on the horizontal surface of the pin and shoulder. The heat can be calculated using Eq. 4

$$Q_{pin1} = \frac{2}{3}(1-\delta)\pi\mu p\omega R_i^3 \quad (4)$$

Heat generated by the friction on the vertical surface of the pin; the local heat can be calculated using Eq. 5:

$$Q_{pin2} = 2\,\pi\,\mu\,p\,\omega L{R_i}^2 \quad (5)$$

where (L_{pin}) is the length of the pin and dependent on the workpiece thickness.

The total friction on heat input by tool pin-welds is the summation of Eq. 4 and 5 as follows

$$Q_{PTotal} = 2\,\pi\mu p\omega R_i^2\left[\frac{(1-\delta)R_i}{3} + L_{pin}\right] \quad (6)$$

3.6 Boundary Conditions

Based on the data from previous studies [43-48], heat loss by convection and radiation was considered in all the workpiece except for the bottom surface because heat loss at the bottom surface occurs by conduction to the backing plate. The heat loss q_s by convection and radiation can be calculated Eq. 7

$$q_s = h(T - T_o) + \varepsilon F\sigma(T^4 - T_o^4) \quad (7)$$

where T is the absolute temperature of the workpiece, T_o is the ambient temperature of the workpiece, h is the convection heat transfer coefficient taken to be 30 W/m^{2}K, ε is the emissivity of surface, taken as 0.5 for aluminum, F is a factor of radiation (1), σ is a Stefan-Boltzmann constant (5.67×10^{-8} W/m^{2}K^4).

On the other hand, heat loss q_{sp} by conduction from the bottom surface of the workpiece can be calculated based literature [18] using Eq. 8

$$q_{sp} = h_p(T - T_o) \quad (8)$$

where h_p is the convection coefficient through the bottom surface; the complexity in determining this coefficient is that the value must be estimated by assuming varying values during a reverse analysis approach. In the model, the optimized value of h_p was taken as 300 W/cm^{2}K. The boundary conditions used in the thermal model are shown in Figure 8.

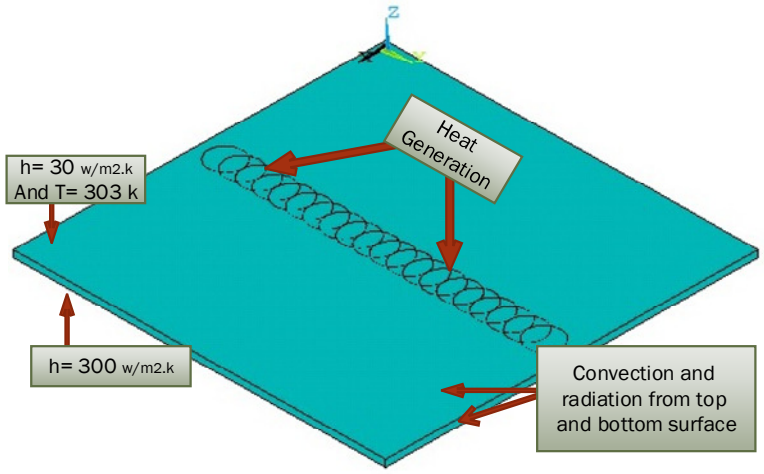

Fig. 8. Schematic of the boundary conditions

3.7 Element Used

In this thermal model, the workpiece was meshed using element SOLID70; it is defined as nodes with temperature as a lone degree of freedom at every node (8), and by orthotropic material properties.

3.8 Simulation

The thermal modeling was implemented using transient thermal analysis. The flow chart of the method used for the finite element analysis was shown in Figure 9.

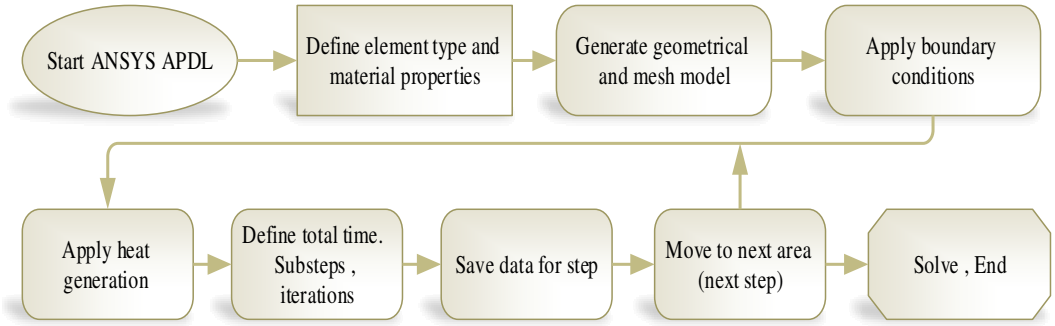

Fig. 9. Flowchart of thermal analysis

4. Results and Discussion

The effect of weld parameters (rotational and welding speed) on the thermal history of 2024-T3 aluminum alloy was studied (simulation and experimentally) and discussed in this section. Figure 10 showed the thermal modeling of the temperature distribution when the tool is moving along the weld centerline for 20 sec. The temperature distribution was influenced by the heat condition between the weld and backing plate; it was also influenced by heat loss through convection and radiation to the environment. The movement speed also influenced the temperature distribution.

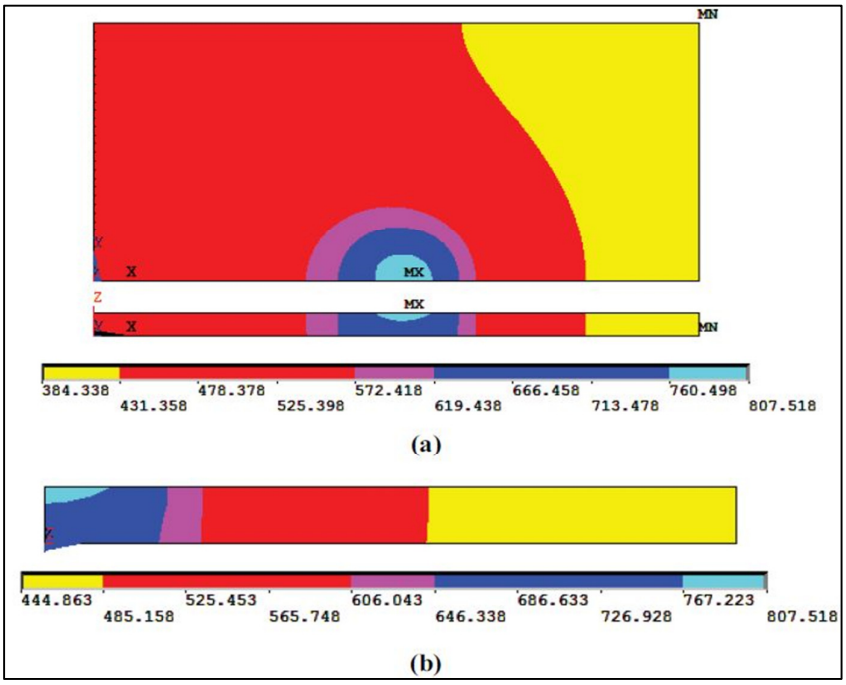

Fig. 10. Temperature distribution (a) on the top, (b) across the welded plate at 20s (690 rpm & 60 mm/min)

4.1 Effect of Rotational Speed

The temperature distribution along the region perpendicular to the center line of the plate welds was shown in Figure 11(a) and (b). It was discovered that an increase in the rotational speed increased the temperature of the plate welds because of the increased frictional heat between the tool-welds interface. Similar results were found by other researchers [35, 36]; moreover, it was discovered from the temperature profile that the maximum temperature was achieved at the stir zone.

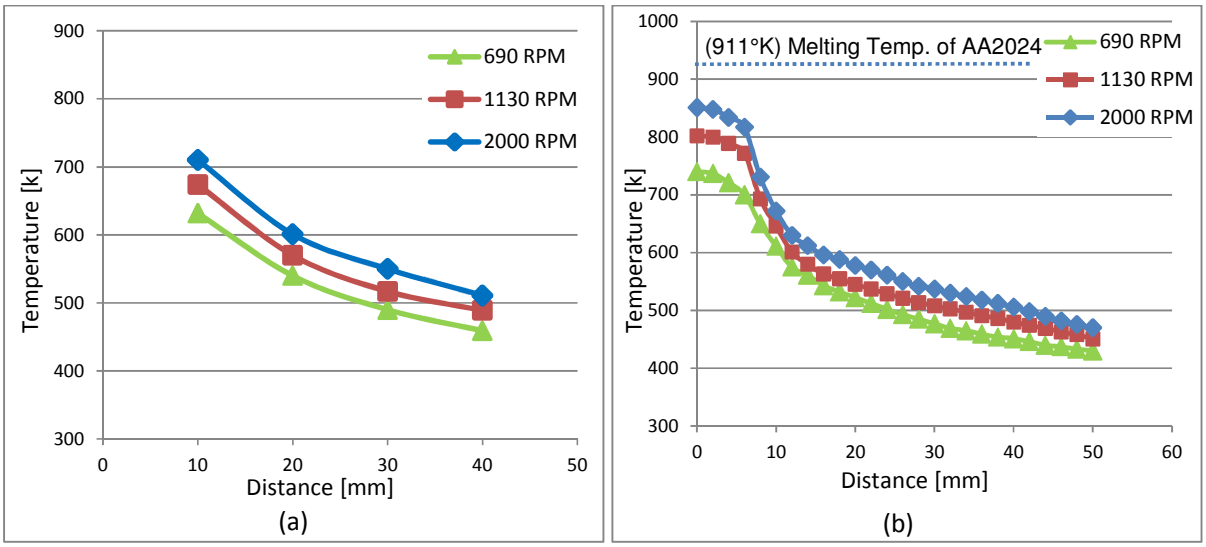

Fig. 11. (a) Experimental, (b) Simulated temperature profiles along the weld at 20 mm/min

Figure 12 showed the comparison of the experimental and simulated temperature values at the welding speed of 20 mm/min along the advancing side from the welds speed. An agreement between the simulated and measured values was observed. Additionally, increases in the rotational speed increased the error ratio as follows: 7.19 % error ratio at X = 10 cm and 2000 rpm, 3.56 % error ratio at X = 10 cm and 690 rpm.

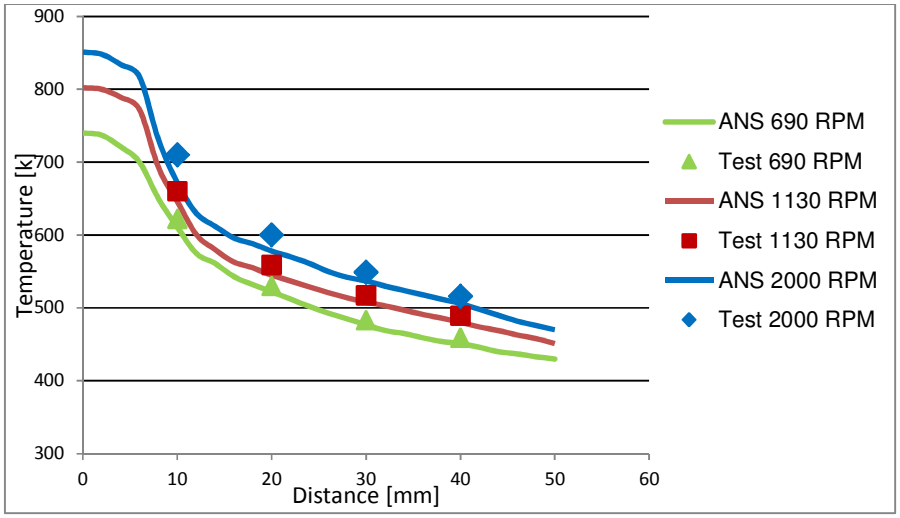

Fig. 12. Comparison of the experimental and simulated temperatures at the welding speed of 20 mm/min

4.2 Effect of welding speed

Figure 13 (a) and (b) showed the temperature distribution along the plate weld. It was observed that increases in the welding speed decreased the temperature due to the decrease in the frictional dwell time. Moreover, the temperature profile for different welding speeds remained the same, indicating a uniform effect of welding speed on temperature along the weld plate. Similar results were reported by Jain *et al.,* [35].

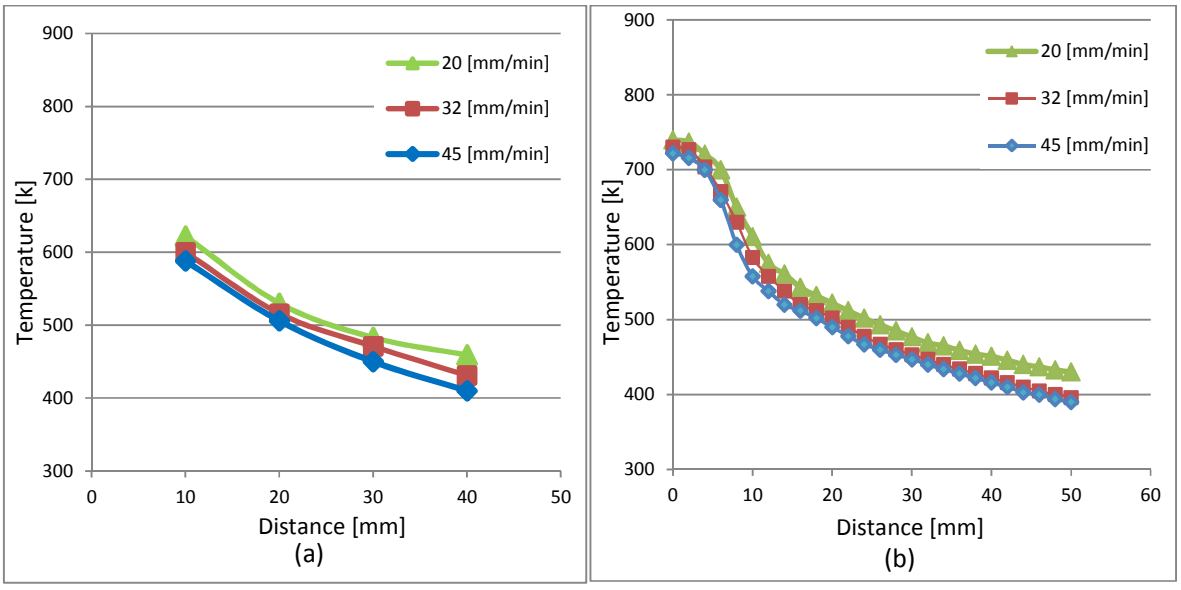

Fig. 13. (a) Experimental, (b) Simulated temperature profiles along the weld at 690 rpm

Figure 14, showed the comparison of the experimental and simulated temperature value at the welding speed of 690 rpm along the advancing side from the weld. An agreement was observed between the simulated and measured values. Additionally, error rates due to increases in the welding speed decreased as follows 7.4 % error ratio at X = 10 cm and 20 mm/min, 3.7 % error ratio at X = 10 cm and 45 mm/min.

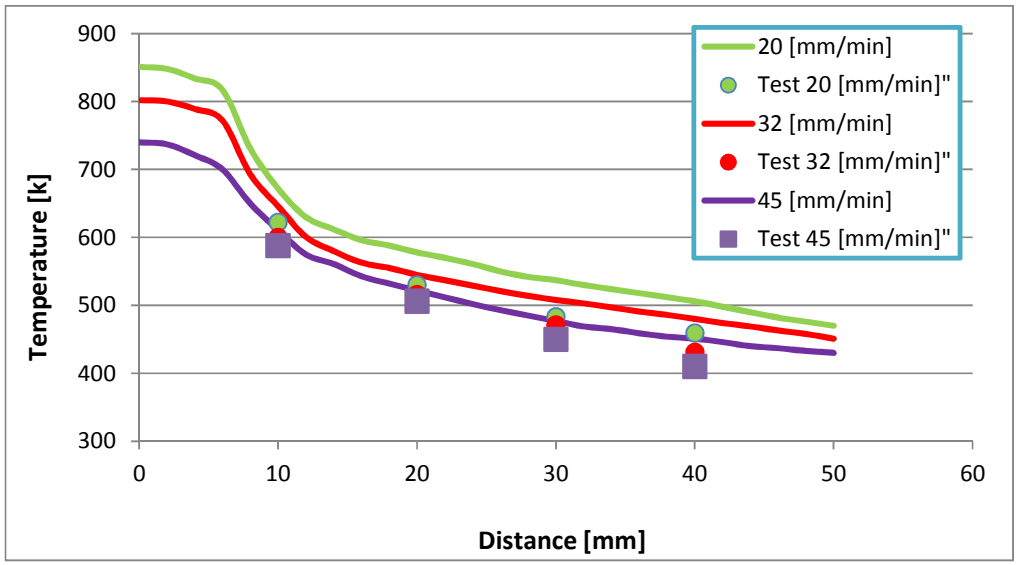

Fig. 14. Comparison of the experimental and simulated temperatures at the welding speed of 690 rpm.

4.3 Effect Rotational and Welding Speed

The heat generated from FSW is estimated by the quotient of the spindle power and welding speed; the spindle power is a function of the rotational speed of the tool. As such, the cumulative influence of rotational speed and welding speed serve as an estimate of the heat generated into the weld. Figure 15 showed the simulated peak temperature at the weld zone for different welding speeds and rotational speeds. The temperature at the center line underneath the tool shoulder was different for different process conditions as follows: least value of 710 K for the weld at 960 rpm and 45 mm/min, and the maximum value of 860 K for the weld at 2000 rpm and 20 mm/min. It is discerning from the plot that the maximum temperature at the weld zone was more affected by rotational speed than welding speed.

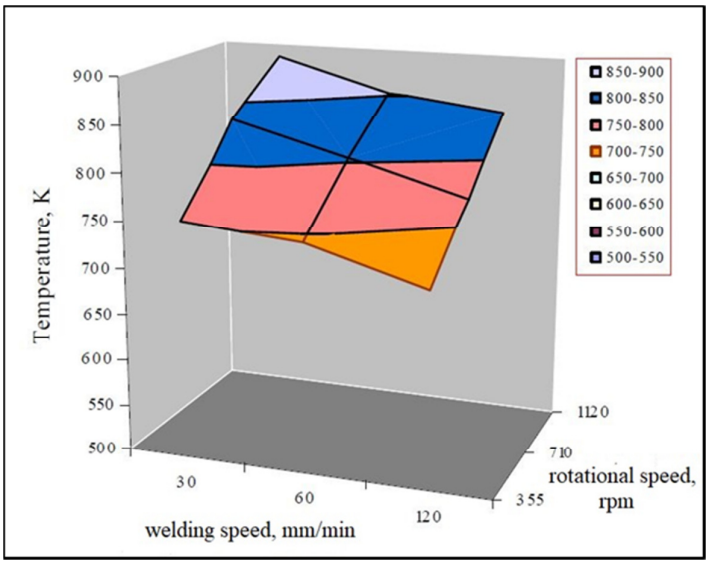

Fig. 15. Simulated peak temperature at the weld zone

5. Conclusion

In this paper, temperature distribution during FSW of AA2024-T3 was evaluated experimentally and numerically for different machine parameters. The experimentally-determined temperature was recorded using a K-type thermocouple fixed perpendicularly to the weld centerline weld while the numerically-determined temperature was estimated using finite element method. The following conclusions were drawn from the results of the study

I. High temperature was observed at 2000 rpm, 20 mm/min, 20 dwell time, and 3° tilt angle since the last observed temperature value was 860 K before the melting of the Al 2024 alloy at 911 K.
II. The numerical results showed that the temperature distribution increased with increases in the rotational speed (T_{max}= 860 K at 2000 rpm & 20 mm/min, and T_{max}= 734 K at 690 rpm & 20 mm/min).
III. The numerical results also showed that the temperature distribution increased with decreases in the welding speed (T_{max}= 710 K at 690 rpm & 45 mm/min, and T_{max}= 734 at 690 rpm & 20 mm/min).

IV. An agreement was found between the experimental and numerical values, with an acceptable error ratio which showed the ability of the model to correctly predict the heat transfer process during FSW.

V. The temperature profile showed that the highest temperature at the stir zone appeared due to influenced by the tool.

Acknowledgment
The authors are grateful to Tikrit University for providing financial support to complete this project.

References

[1] M.H. Zaidan, H.J. Khalaf, B.A. Ahmed. "Thermal analysis of a solar absorption cooling system with hot and cold storage tanks", *Journal of Advanced Research in Fluid Mechanics and Thermal Sciences* 50 (2018): 67-80.

[2] A.A. Razali, A. Sadikin, S. Ayop. "Structural analysis and morphological study of Al_2O_3 nanofluids in microchannel heat sink", *Journal of Advanced Research in Fluid Mechanics and Thermal Sciences* 46 (2018): 139-146.

[3] M.A. Othuman Mydin, O. Mydin, M. Nasrun, M. Nawi, M.A. C. Munaaim, C. Munaaim, N. Mohamad, A. Aziz, A.A. Abdul Samad, I. Johari, P. "Effect of Steel Fibre Volume Fraction on Thermal Performance of Lightweight Foamed Mortar (LFM) at Ambient Temperature", *Journal of Advanced Research in Fluid Mechanics and Thermal Sciences* 47 (2018): 119-126

[4] Kashaev, Nikolai, Volker Ventzke, and Gürel Çam. "Prospects of laser beam welding and friction stir welding processes for aluminum airframe structural applications." *Journal of Manufacturing Processes* 36 (2018): 571-600.

[5] Al-Sammarraie, Ahmed Tawfeeq Ahmed, and Manar Salih Mahdi. "Theoretical Study of Heat Transfer through a Sun Space Filled with a Porous Medium." *Tikrit Journal of Engineering Sciences* 23, no. 2 (2016): 10-20.

[6] Al-Sammarraie, Ahmed Tawfeeq Ahmed. "Natural Convection Heat Transfer from Two Parallel Horizontal Cylinders Embedded in a Porous Medium inside a Horizontal Cylindrical Enclosure." *Wulfenia J* 20, no. 3 (2013): 118-134.

[7] Al-Sammarraie, Ahmed Tawfeeq Ahmed, Raaid Rashad Jassem, and Thamir K. Ibrahim. "Mixed Convection Heat Transfer in Inclined Tubes with Constant Heat Flux." *European Journal of Scientific Research* 97, no. 1 (2013): 144-158.

[8] Al-Sammarraie, Ahmed T., and Kambiz Vafai. "Heat transfer augmentation through convergence angles in a pipe." *Numerical Heat Transfer, Part A: Applications* 72, no. 3 (2017): 197-214.

[9] Salimpour, Mohammad Reza, Ahmed T. Al-Sammarraie, Azadeh Forouzandeh, and Mahsa Farzaneh. "Constructal design of circular multilayer microchannel heat sinks." *Journal of Thermal Science and Engineering Applications* 11, no. 1 (2019): 011001.

[10] Li, Na, Wenya Li, Xiawei Yang, Yaxin Xu, and Achilles Vairis. "Corrosion characteristics and wear performance of cold sprayed coatings of reinforced Al deposited onto friction stir welded AA2024-T3 joints." *Surface and Coatings Technology* 349 (2018): 1069-1076.

[11] Alkumait, Aadel Abdul Razzaq, Maki Haj Zaidan, and Thamir Khalil Ibrahim. "Akademia Baru." *Journal of Advanced Research in Fluid Mechanics and Thermal Sciences* 52, no. 1 (2018): 33-45.

[12] Elghool, Ali, Firdaus Basrawi, Thamir Khalil Ibrahim, Khairul Habib, Hassan Ibrahim, and Daing Mohamad Nafiz Daing Idris. "A review on heat sink for thermo-electric power generation: Classifications and parameters affecting performance." *Energy conversion and management* 134 (2017): 260-277.

[13] Zaidan, Maki H., Aadel AR Alkumait, and Thamir K. Ibrahim. "Assessment of heat transfer and fluid flow characteristics within finned flat tube." *Case studies in thermal engineering* 12 (2018): 557-562.

[14] Mohammed, Mohammed K., M. Kh Abdolbaqi, Thamir K. Ibrahim, Rizalman Bin Mamat, and Omar I. Awad. "Experimental and Numerical investigation of Heat transfer enhancement using Al2O3-Ethylene Glycol/Water nanofluids in straight channel." In *MATEC Web of Conferences*, vol. 225, p. 01019. EDP Sciences, 2018.

[15] Mhamuad, Aziz7 M., Thamir Kh Ibrahim, and Raid R. Jasim. "Determination of the temperature distribution the perforated fins under." *Tikrit Journal of Engineering Sciences* 15, no. 2 (2008): 63-78.

[16] Ibrahim, Thamir K., Mohammed Marwah Noori, and Ibrahim Hassan. "Effect of perforation area on temperature distribution of the rectangular fins under natural convection." *ARPN Journal of Engineering and Applied Sciences* 11, no. 10 (2016): 6371-6375.

[17] Li, N., W. Y. Li, X. W. Yang, Y. Feng, and A. Vairis. "An investigation into the mechanism for enhanced mechanical properties in friction stir welded AA2024-T3 joints coated with cold spraying." *Applied Surface Science* 439 (2018): 623-631.

[18] Ibrahim, Thamir K. "The Life cycle assessments of gas turbine using inlet air cooling system." *Tikrit Journal of Engineering Sciences* 22, no. 1 (2015): 69-75.
[19] Ibrahim, Thamir K., Marwah N. Mohammed, Mohammed Kamil Mohammed, G. Najafi, Nor Azwadi Che Sidik, Firdaus Basrawi, Ahmed N. Abdalla, and S. S. Hoseini. "Experimental study on the effect of perforations shapes on vertical heated fins performance under forced convection heat transfer." *International Journal of Heat and Mass Transfer* 118 (2018): 832-846.
[20] Ibrahim, Thamir K., and M. M. Rahman. "Optimum performance improvements of the combined cycle based on an intercooler–reheated gas turbine." *Journal of Energy Resources Technology* 137, no. 6 (2015): 061601.
[21] Trimble, D., G. E. O'Donnell, and J. Monaghan. "Characterisation of tool shape and rotational speed for increased speed during friction stir welding of AA2024-T3." *Journal of Manufacturing processes* 17 (2015): 141-150.
[22] Li, W. Y., N. Li, X. W. Yang, Y. Feng, and A. Vairis. "Impact of cold spraying on microstructure and mechanical properties of optimized friction stir welded AA2024-T3 joint." *Materials Science and Engineering: A* 702 (2017): 73-80.
[23] Ahmed, Mahmood H. Ali Ahmed Tawfiq, and Khalaf Ibraheem Hamada. "Numerical Study of Non-Darcian Natural Convection Heat Transfer in a Rectangular Enclosure Filled with Porous Medium Saturated with Viscous Fluid." *Tikrit Journal of Engineering Sciences* 15, no. 2 (2008): 90-111.
[24] Mohammed, Mohammed Kamil, Omar I. Awad, M. M. Rahman, G. Najafi, Firdaus Basrawi, Ahmed N. Abd Alla, and Rizalman Mamat. "The optimum performance of the combined cycle power plant: A comprehensive review." *Renewable and Sustainable Energy Reviews* 79 (2017): 459-474.
[25] Ibrahim, Thamir K., and M. M. Rahman. "Parametric simulation of triple-pressure reheat combined cycle: A case study." *Advanced Science Letters* 13, no. 1 (2012): 263-268.
[26] Abdalla, Ahmed N., Omar I. Awad, Hai Tao, Thamir K. Ibrahim, Rizalman Mamat, and Ali Thaeer Hammid. "Performance and emissions of gasoline blended with fusel oil that a potential using as an octane enhancer." *Energy Sources, Part A: Recovery, Utilization, and Environmental Effects* (2018): 1-17.
[27] Ibrahim, Thamir K., and M. M. Rahman. "Effect of compression ratio on the performance of different strategies for the gas turbine." *International Journal of Automotive and Mechanical Engineering* 9 (2014): 1747.
[28] Avinash, P., M. Manikandan, N. Arivazhagan, K. Devendranath Ramkumar, and S. Narayanan. "Friction stir welded butt joints of AA2024 T3 and AA7075 T6 aluminum alloys." *Procedia Engineering* 75 (2014): 98-102.
[29] Zapata, J., M. Toro, and D. López. "Residual stresses in friction stir dissimilar welding of aluminum alloys." *Journal of Materials Processing Technology* 229 (2016): 121-127.
[30] Song, M., and R. Kovacevic. "Thermal modeling of friction stir welding in a moving coordinate system and its validation." *International Journal of Machine Tools and Manufacture* 43, no. 6 (2003): 605-615.
[31] Aval, H. Jamshidi, S. Serajzadeh, and A. H. Kokabi. "Theoretical and experimental investigation into friction stir welding of AA 5086." *The International Journal of Advanced Manufacturing Technology* 52, no. 5-8 (2011): 531-544.
[32] Muhsin, J. J., Moneer H. Tolephih, and A. M. Muhammed. "Effect of friction stir welding parameters (rotation and transverse) speed on the transient temperature distribution in friction stir welding of AA 7020-T53." *ARPN Journal of Engineering and Applied Sciences* 7, no. 4 (2012): 436-446.
[33] Padmanaban, R. V. R. K., V. Ratna Kishore, and V. Balusamy. "Numerical simulation of temperature distribution and material flow during friction stir welding of dissimilar aluminum alloys." *Procedia Engineering* 97 (2014): 854-863.
[34] Ghetiya, N. D., K. M. Patel, and Anup B. Patel. "Prediction of temperature at weldline in air and immersed friction stir welding and its experimental validation." *The International Journal of Advanced Manufacturing Technology* 79, no. 5-8 (2015): 1239-1246.
[35] Jain, Rahul, Surjya Kanta Pal, and Shiv Brat Singh. "Finite element simulation of temperature and strain distribution during friction stir welding of AA2024 aluminum alloy." *Journal of The Institution of Engineers (India): Series C* 98, no. 1 (2017): 37-43.
[36] Aziz, Saad B., Mohammad W. Dewan, Daniel J. Huggett, Muhammad A. Wahab, Ayman M. Okeil, and T. Warren Liao. "Impact of Friction Stir Welding (FSW) process parameters on thermal modeling and heat generation of aluminum alloy joints." *Acta Metallurgica Sinica (English Letters)* 29, no. 9 (2016): 869-883.
[37] Verma, S., and J. P. Misra. "Study on temperature distribution during Friction Stir Welding of 6082 aluminum alloy." *Materials Today: Proceedings* 4, no. 2 (2017): 1350-1356.
[38] Fathinia, F., and Ahmed Kadhim Hussein. "Effect of Blockage Shape on Unsteady Mixed Convective Nanofluid Flow Over Backward Facing Step." *CFD Letters* 10 (2018): 1-18.
[39] Ji, Yingchun. "CFD modelling of natural convection in air cavities." *CFD Letters* 6, no. 1 (2014): 15-31.
[40] Cheng, See-Yuan, Shuhaimi Mansor, Mohd Azman Abdullah, and Mohamad Shukri Zakaria. "Akademia Baru." *Journal of Advanced Research in Fluid Mechanics and Thermal Sciences* 47, no. 1 (2018): 108-118.

[41] Yang, C. L., C. S. Wu, and L. Shi. "Analysis of friction reduction effect due to ultrasonic vibration exerted in friction stir welding." *Journal of Manufacturing Processes 35* (2018): 118-126.
[42] Dixon, John, Douglas Burkes, and Pavel Medvedev. "Thermal modeling of a friction bonding process." In *Proceedings of the COMSOL Conference,* pp. 349-354. 2007.
[43] Ibrahim, Thamir K., and M. M. Rahman. "Effective Parameters on Performance of Multipressure Combined Cycle Power Plants." *Advances in Mechanical Engineering (Hindawi Publishing Corporation)* (2014).
[44] Shaysultanov, D., N. Stepanov, S. Malopheyev, I. Vysotskiy, V. Sanin, S. Mironov, R. Kaibyshev, G. Salishchev, and S. Zherebtsov. "Friction stir welding of a carbon-doped CoCrFeNiMn high-entropy alloy." *Materials Characterization* 145 (2018): 353-361.
[45] Ilman, M. N., and P. T. Iswanto. "Fatigue crack growth rate behaviour of friction-stir aluminium alloy AA2024-T3 welds under transient thermal tensioning." *Materials & Design* 50 (2013): 235-243.
[46] El-Sayed, M. M., A. Y. Shash, and M. Abd-Rabou. "Finite element modeling of aluminum alloy AA5083-O friction stir welding process." *Journal of Materials Processing Technology* 252 (2018): 13-24.
[47] Mustafa, W.A., Saidi, S.A., Zainal, M., Santiagoo, R. "Experimental Study of Composites Material Based on Thermal Analysis", *Journal of Advanced Research in Fluid Mechanics and Thermal Sciences* 43(2018): 37-44.
[48] M. Zainal, Z. Aihsan, W. Mustafa, R. Santiagoo, P." Experimental Study on Thermal and Tensile Properties on Polypropylene Maleic Anhydride as a Compatibilizer in Polypropylene/Sugarcane Bagasse Composite", *Journal of Advanced Research in Fluid Mechanics and Thermal Sciences* 43 (2018): 141-148.